Pis'ma v ZhETF, vol.70, iss.10, pp.680 - 683

LOW-TEMPERATURE MAGNETIC PROPERTIES OF 2D MOLECULAR FERRIMAGNET $N(n\text{-}C_5H_{11})_4[Fe^{II}Fe^{III}(C_2O_4)_3]$

L.Bottyán, L.Kiss+, N.S.Ovanesyan[1)], A.A.Pyalling, N.A.Sanina*, A.B.Kashuba[Δ]*

KFKI, Research Institute for Particle and Nuclear Physics
1525 Budapest, P.O.B. 49 Hungary

+Institute for Solid State Physics and Optics
1525 Budapest, P.O.B. 49 Hungary

**Institute of Problems of Chemical Physics RAS*
142432 Chernogolovka, Moskow reg., Russia

[Δ]L.D.Landau Institute for Theoretical Physics RAS
142432 Chernogolovka, Moskow reg., Russia

Submitted 14 October 1999

^{57}Fe Mössbauer and magnetometric studies of molecular ferrimagnet $N(n\text{-}C_5H_{11})_4[Fe^{II}Fe^{III}(C_2O_4)_3]$ are indicative of a 2D magnetic character with strong uniaxial anisotropy in the crystal's basal plane. It is established that the change in the sign of the net magnetization of this compound is related to a compensation between Fe^{III} and Fe^{II} sublattice magnetizations at $T_{comp} = 31.2$ K. The form and parameters of the magnetic Hamiltonian describing the temperature dependence of the Fe^{III} sublattice and the net magnetizations has been determined.

PACS: 75.50.Gg, 76.80.+y

In search for new molecular magnets, considerable attention has been paid in the last decade to the synthesis of bimetallic transition metal complexes with spontaneous magnetization. Okawa et al. suggested the use of *tris*-oxalate of chromium $[Cr^{III}(ox)_3]^{3-}$ and iron $[Fe^{III}(ox)_3]^{3-}$ with D_3-symmetry as building blocks (ox=$(C_2O_4)^{2-}$). This kind of synthesis led to a discovery of a whole family of ferromagnetic and ferrimagnetic materials of the form $NBu_4[M^{II}M^{III}(ox)_3]$, where M^{II} =Mn, Fe, Co, Ni, Cu; Bu= n-C_4H_9 [1,2]. These and similar compounds with different organic cations crystallize in a trigonal structure with space group $R3c$ [3,4]. The honeycomb-like 2D lattice with the two different magnetic ions in the corners of the hexagon form alternating layers $[M^{II}M^{III}(ox)_3]_n^{n-}$ separated by the organic cations. In such a structure, ferro and ferrimagnetism are both feasible by the intralayer superexchange interaction along $M^{II}-(ox)^{2-}-M^{III}$ path. The inter-layer interaction is weak due to the considerable distance between layers, dependent on the organic cation (d = 8 to 15 Å [5,6]). Consequently, a stack of two-dimensional magnets is a good representation for such compounds.

Here we report on Mössbauer and magnetometric investigations of ferrimagnetic $NPn_4[Fe^{II}Fe^{III}(ox)_3]$, where Pn= n-C_5H_{11}, in the temperature range 4.2 − 100 K (the Néel temperature T_N = 48 K). Particular interest in this compound is related to the reported negative sign of magnetization [7]. We have fitted temperature dependencies of the Fe^{III} and Fe^{II} sublattice magnetizations in the frame of a relevant microscopic model

[1)] e-mail: ovanesyan@icp.ac.ru

and have determined an exchange constant, magnetic anisotropy constants and the g-factor of Fe^{II}. It is shown that this compound is an N-type ferrimagnet according to the classification by Néel [8].

The polycrystalline compound was synthesized by the standard method [6]. Magnetization measurements were performed by a Quantum Design MPMS-5S SQUID magnetometer in *rso* mode with external magnetic fields and temperature range of 1 mT to 5 T and 5 to 100 K, respectively. The powder specimen of 58 mg was compacted into the sample holder. ^{57}Fe Mössbauer spectra were recorded at various temperatures using a He gas-flow cryostat of type CF506 (Oxford Instruments).

The basic distortion of the coordination octahedron in the metal-oxalate layers of $NPn_4[Fe^{II}Fe^{III}(ox)_3]$ is the compression along the trigonal axis, parallel to the crystallographic c-axis. In addition, a small rhombic distortion is present reducing the space group from $R3c$ to $C222_1$ and the site symmetry of both Fe^{II} and Fe^{III} from D_3 to C_2 [9]. The distance between nearest (Fe^{II} and Fe^{III}) ions in neighboring layers is $d = 10.23$ Å [5].

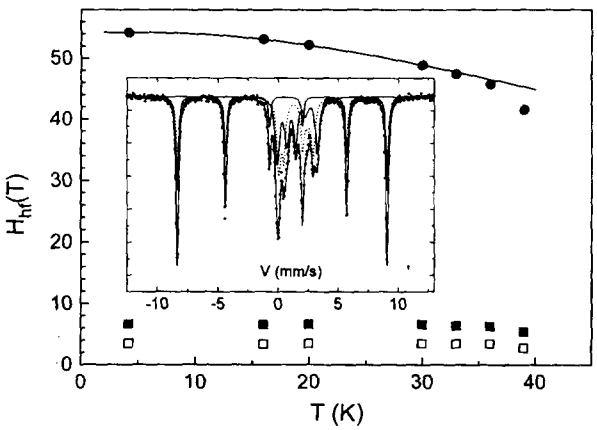

Fig.1. Temperature dependencies of Fe^{III} (•) and two Fe^{II} (■ and □) hyperfine fields in $NPn_4[Fe^{II}Fe^{III}(ox)_3]$. The solid line represents the Fe^{III} magnetization derived from the model Hamiltonian (1). The inset shows an example Mössbauer spectrum at 4.2 K fitted with combined magnetic-quadrupole hyperfine full Hamiltonian

^{57}Fe Mössbauer spectrum of the compound at $T = 4.2$ K is displayed in the inset of Fig.1. It shows the magnetic hyperfine structure of $Fe^{III}(S = 5/2)$ and $Fe^{II}(S = 2)$ ions with an intensity ratio of 1:1. The spectra are analyzed in terms of the electron-nuclear Hamiltonian including magnetic hyperfine and electric quadrupole interactions. We find a *negative* z-component of the electric field gradient (EFG) V_{zz} at Fe^{II}, which corresponds to the trigonal comression of the oxygen octahedron along the c-axis, and a non-zero asymmetry parameter $(V_{xx} - V_{yy})/V_{zz} \leq 0$ which manifests the rhombic distortion. The angles, θ^{II} and θ^{III} between the principal z-direction of the EFG and the hyperfine fields at the nuclei of Fe^{II} and Fe^{III} are both 90°, i.e. the magnetization is confined to the basal plane of the crystal. The hyperfine field, H_{hf}, at the nucleus of Fe^{II} is considerably lowered due to a significant unquenched orbital moment contribution [10]. Moreover, there exist two nonequivalent sites for Fe^{II} ion as indicated by two slightly different values of H_{hf} in Fig.1. The intensity ratio of the Mössbauer lines corresponds to a random orientation of the easy axes of magnetization of the crystallites in the polycrystalline sample.

Temperature dependence of the hyperfine fields, $H_{hf}(T)$, at Fe^{II} and Fe^{III} is shown in Fig.1. H_{hf} at Fe^{II} site is practically temperature independent, an indication of an identical temperature dependence of the spin and orbital components of the magnetic moment. In order to describe the temperature dependence $H_{hf}(T)$ at Fe^{III} site (proportional to the

Fe^{III} sublattice magnetization), the following form of the 2D microscopic Hamiltonian of a single layer of $NPn_4[Fe^{II}Fe^{III}(ox)_3]$ is assumed:

$$\hat{H} = J\sum_{ab}\mathbf{S}_a\mathbf{S}_b + \frac{\lambda_z}{2}\sum_b (S_b^z)^2 + \frac{\lambda_y}{2}\sum_b (S_b^y)^2 - 2\mu_B\sum_a \mathbf{S}_a\mathbf{H} - g_b\mu_B\sum_b \mathbf{S}_b\mathbf{H} \qquad (1)$$

where the indices a and b run on the Fe^{III} and Fe^{II} sublattices, respectively. We have estimated a variation of the parameters in the Hamiltonian (1) for the two nonequivalent Fe^{II} sites as being negligible.

The first term of Hamiltonian (1) is the antiferromagnetic exchange interaction of strength J. The second and third terms of the Hamiltonian describe the magnetic anisotropy on the Fe^{II} sublattice, due to the orbital moment of the Fe^{II} ion [7]. The magnetic anisotropy at the Fe^{III} site is neglected, since its orbital moment $L = 0$. The last two terms are the Zeeman-interactions with the external field. For the Fe^{III} ion, the g-factor has the value of 2. By standard Holstein–Primakoff transformation, an effective spin-wave Hamiltonian is obtained from (1). Neglecting the interaction between spin waves, the temperature dependence of the magnetization of both sub-lattices was calculated. The best agreement with the Fe^{III} experimental $H_{hf}(T)$ data is achieved with the following values of the parameters in the Hamiltonian (1):

$$J = 12.4(2)\,\mathrm{K}, \quad \lambda_y = 9.6(8)\,\mathrm{K}, \quad \lambda_z = 20 - 50\,\mathrm{K}. \qquad (2)$$

The value of the λ_z parameter has little effect on the Fe^{III} magnetization.

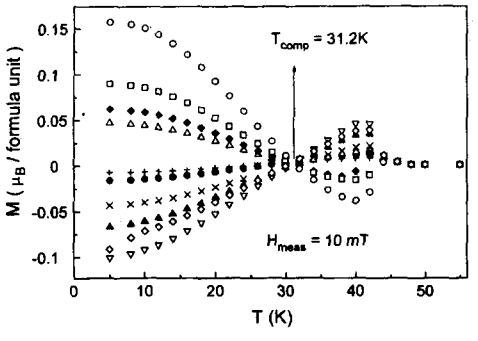

Fig.2. Temperature dependence of the net magnetization as measured by SQUID in $NPn_4[Fe^{II}Fe^{III}(ox)_3]$ cooled in various external magnetic fields: 15 mT(+), 20 mT(•), 50 mT(◇), 0.1 T(▽), 0.2 T(▲), 0.5 T(×), 0.8 T(△), 1 T(♦), 2 T(□) and 5 T(○). The measuring field was 10 mT, throughout

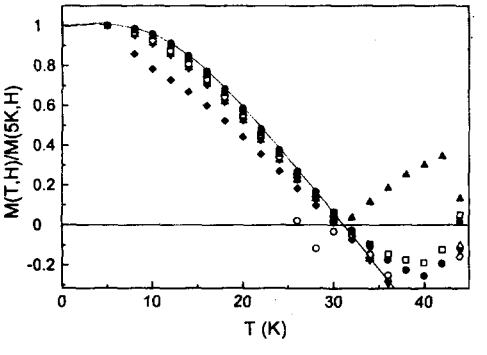

Fig.3. Normalized magnetization curves of $NPn_4[Fe^{II}Fe^{III}(ox)_3]$ cooled to 5 K in external magnetic fields ranging from 50mT(+) to 5 T(○). Solid line represents a fitting curve derived from Hamiltonian (1) with parameters (2) and g_b = = 2.34(2)

SQUID magnetometry of the sample was performed in the following way. First, the sample was cooled from $T = 100\,\mathrm{K}$ to $T = 5\,\mathrm{K}$ in external magnetic fields ranging from $H = 1$ mT to $H = 5\,\mathrm{T}$, and then the magnetization, $M(T, H)$ (where H is the cooling field) was recorded in a measuring field: $H_{meas} = 10\,\mathrm{mT}$, as a function of increasing temperature. Experimental results are displayed in Fig.2, with two features being prominent. First, the magnetization of the sample changes sign at around $T_{comp} = 31.2\,\mathrm{K}$. Second, the polycrystalline specimen did not reach magnetic saturation at 5 K and hence it is frozen

in a magnetically metastable state with a certain domain structure. Those domains that coincide with crystallites of specimen do hold their magnetic orientation upon heating even if the direction of their magnetization is opposite to H_{meas}. The net magnetization of such a domain follows a *microscopic* magnetization $M(T)$. In the case of a specimen having single domain structure within each crystallite, one can extract this microscopic magnetization $M(T)$ by normalizing the magnetization curve to its value at $T = 0$. We plotted seven normalized curves $M(T,H)/M(5\,\mathrm{K},H)$ for seven cooling magnetic fields: 5 T, 2 T, 0.8 T, 0.5 T, 0.2 T, 0.1 T and 50 mT, in Fig.3. The magnetization curve $M(T)$ for a magnet described by Hamiltonian (1) was calculated with the parameters (2) leaving the Fe^{II} g-factor variable during fit. The solid line shown in Fig.3 was achived with $g_b = 2.34(2)$. Note, that $M(T,H)/M(5\,\mathrm{K},H)$ curves for strong cooling fields approach a limiting curve which we identify with the microscopic $M(T)$. In order to cross-examine this result we calculated a saturation magnetization for our specimen, assuming random directions of the c-axis in crystallites, to be $M(0) = 0.16(2)\mu_B$ per Fe^{III}–Fe^{II} pair.

On the other hand, a considerable deviation of $M(T,H)/M(5\,\mathrm{K},H)$ curves for weaker cooling fields from $M(T)$ can be interpreted as 'freezing-out' of the movement of domain walls within crystallites. We mention also that in two cooling fields, 0.5 T and 0.2 T, the dc and rso signals of the experimental curves $M(T,H)$ are not identical below T_{comp}. The apparent convergence of all $M(T,H)/M(5\,\mathrm{K},H)$ curves in the vicinity of T_{comp} illustrate the fact that two domains of opposite order parameter have identical magnetization at T_{comp}.

We suggest that in the cooling fields $H > 0.1$ T and for $T < T_{comp}$ the sample is magnetized up to its equilibrium magnetization. In rather strong cooling fields $H > 0.8$ T most single domain crystallites reverse their magnetization during the cooling below T_{comp}, whereas in weaker cooling fields $H < 0.8$ T only few crystallites reverse their magnetization completely leaving many domain walls inside the crystallites to the end of the cooling at 5 K. In very weak cooling fields $H < 0.1$ T the crystallites do not reach magnetic saturation even at $T > T_{comp}$ and with decreasing cooling fields, the magnetization of the sample decreases. Recent external magnetic field Mössbauer experiments have shown that even $H_{ext} = 7$ T is not sufficient to polarize the powder sample [11]. This result is again in agreement with large value of the fitted anisotropy constants, λ_y and λ_z, and large orbital contribution to H_{hf} on Fe^{II}.

This work was partially supported by the Hungarian Scientific Research Fund (OTKA) under contract T022559 and Russian Foundation for Basic Research, project 99-03-32581.

---

1. H.Tamaki, Z.J.Zhong, N.Matsumoto et al., J. Am. Chem. Soc. **114**, 6974 (1992).
2. H.Okawa, N.Matsumoto, H.Tamaki, and M.Ohba, Mol. Cryst. Liq. Cryst. **233**, 257 (1993).
3. L.O.Atovmyan, G.V.Shilov, R.N.Lyubovskaya et al., JETP Lett. **58**, 766 (1993).
4. S.Decurtins, H.W.Schmale, H.R.Oswald et al., Inorg. Chim. Acta **216**, 65 (1994).
5. C.Mathoniere, C.J.Nutall, S.G.Carling, and P.Day, Inorg.Chem. **35**, 1201 (1996).
6. G.V.Shilov, L.O.Atovmyan, N.S.Ovanesyan et al., Russian J. Coord. Chem. **24**, 288 (1998).
7. C.J.Nutall and P.Day, Chem.Mater, **10**, 3050 (1998).
8. J.L.Néel, Ann. Phys. (Paris) **3**, 137 (1948).
9. S.G.Carling, C.Mathoniere, P. Day et al., J. Chem. Soc., Dalton Trans. 1839 (1996).
10. N.S.Ovanesyan, G.V.Shilov, L.O.Atovmyan et al., Mol. Cryst. Liq. Cryst. **273**, 175 (1995).
11. N.S.Ovanesyan, G.V.Shilov, N.A.Sanina et al., Mol. Cryst Liq. Cryst. (1999), in press.